THE EUROPEAN
PHYSICAL JOURNAL C

Regular Article - Theoretical Physics

Constraints on interacting dark energy models through cosmic chronometers and Gaussian process

Muhsin Aljaf[1,2,a] ⓘ, **Daniele Gregoris**[3,4,5,b] ⓘ, **Martiros Khurshudyan**[6,7,8,c] ⓘ

[1] Department of Astronomy, University of Science and Technology of China, Hefei 230026, Anhui, China
[2] Department of Physics, College of Education, University of Garmian, Kalar, Kurdistan Region, Iraq
[3] School of Science, Jiangsu University of Science and Technology, Zhenjiang 212003, China
[4] Center for Gravitation and Cosmology, College of Physical Science and Technology, Yangzhou University, 180 Siwangting Road, Yangzhou 225002, Jiangsu, China
[5] School of Aeronautics and Astronautics, Shanghai Jiao Tong University, Shanghai 200240, China
[6] Institute of Physics, University of Silesia, Katowice, Poland
[7] Consejo Superior de Investigaciones Cientcas, ICE/CSIC-IEEC, Campus UAB, Carrer de Can Magrans s/n, 08193 Bellaterra, Barcelona, Spain
[8] International Laboratory for Theoretical Cosmology, Tomsk State University of Control Systems and Radioelectronics (TUSUR), 634050 Tomsk, Russia

Abstract In this paper, after reconstructing the redshift evolution of the Hubble function by adopting Gaussian process techniques, we estimate the best-fit parameters for some flat Friedmann cosmological models based on a modified Chaplygin gas interacting with dark matter. In fact, the expansion history of the Universe will be investigated because passively evolving galaxies constitute cosmic chronometers. An estimate for the present-day values of the deceleration parameter, adiabatic speed of sound within the dark energy fluid, effective dark energy, and dark matter equation of state parameters is provided. By this, we mean that the interaction term between the two dark fluids, which breaks the Bianchi symmetries, will be interpreted as an effective contribution to the dark matter pressure similarly to the framework of the "Generalized Dark Matter". We investigate whether the estimates of the Hubble constant and of the present-day abundance of dark matter are sensitive to the dark matter–dark energy coupling. We will also show that the cosmic chronometers data favor a cold dark matter, and that our findings are in agreement with the Le Châtelier–Braun principle according to which dark energy should decay into dark matter.

1 Introduction

Despite being introduced for addressing a galactic puzzle, i.e., the flattening of the rotation curves, on cosmological scales dark matter combined together with dark energy can account for almost the full energy budget of the Universe. While there are still no experimental devices for confirming the existence of dark energy directly, the situation seems to be different for dark matter thanks to the model-independent study of its distribution within the Milky Way [1]. In the simplest cosmological scenario, the ΛColdDarkMatter (ΛCDM) model, dark matter is macroscopically pictured as a pressureless fluid [2]. However, different microscopic foundations for dark matter have been proposed linking it to some fundamental elementary particle theories like those of massive neutrinos [3], sterile neutrinos [4], axions [5], axinos [6], gravitinos [7], and neutralinos [8], just to mention a few examples (for a review of the different proposals of dark matter modelings in terms of elementary particles beyond the standard model, and how they affect the possible detection methods see [9,10]). However, massive neutrinos may not explain the formation of large-scale structures [11,12], while, on the other hand, sterile neutrinos and axions are consistent with the CP violation [13,14]. Furthermore, a detection of dark matter constituted of axinos, gravitinos, or neutralinos can lead to an experimental confirmation of supersymmetric field theories [15]. Microscopically, the possible different modelings of dark matter can be classified into hot (with the massive neutrinos being one example), warm (as for sterile neutrinos), and cold (like for axions and neutralinos) depending on the

a e-mail: mohsen@mail.ustc.edu.cn

b e-mail: danielegregoris@libero.it (corresponding author)

c e-mail: khurshudyan@ice.csic.es

energy scale of the elementary particles constituting this fluid [2].

The aforementioned ΛColdDarkMatter model assumes a dark energy fluid equivalent to a cosmological constant term entering the Einstein field equations, and that the two dark fluids are separately conserved, i.e., that they do not interact with each other through any energy exchange. A consistent joint interpretation of Planck results and weak lensing data however suggests that some redshift evolution of the dark energy equation of state parameter may be necessary [16, Sect.6.3]. Furthermore, interactions between dark energy and dark matter can alleviate the coincidence problem [17–20], and mitigate the discrepancies between the estimates of the Hubble constant from cosmic microwave background measurements or large scale structures versus supernovae data as argued in [21,22]; we refer as well to [23–40] for quantitative analyses on whether energy flows between dark matter and dark energy affect the estimates of various cosmological parameters. Complementary studies have investigated how the growth of instabilities in interacting dark models affects the formation of astrophysical structures [41–48], such as primordial black holes [49–51], and galactic halos [52–62] due to the fact that the density of dark matter does not dilute any longer with the cube of the scale factor of the universe. Gravitational waves has been used for constraining dark interactions as well [63–66]. Moreover, a coupling between the dark energy field and dark matter, with the latter pictured as neutrinos, affects the neutrinos' masses estimates [67–69]. From a more mathematical point of view, specific interplays between the equation of state of dark energy and the interaction term with dark matter can give rise to different types of finite-time kinematic and matter density singularities [70,71].

For taking into account the observational requirement of an evolving equation of state of dark energy, we model the dark energy fluid as a modified Chaplygin gas [72,73], rather than considering just a redshift parametrization [74,75], because of its well established physical motivation. In fact, this fluid approach belongs to the wider class of chameleon field theories in which the constant equation of state parameter $p = w\rho$ is promoted to an energy-dependent functional according to $w \rightarrow w(\rho)$, and therefore it exhibits a sort of running [76,77]. In particular, our fluid model interpolates between an ideal fluid behavior at low energy densities and a generalized Chaplygin gas in the high energy limit. Therefore, we implement a sort of *asymptotic freedom* at low energies because the interactions within the fluid are suppressed [78,79], while at high energies, we match with the Born–Infeld paradigm with our model being formulated in terms of the Nambu–Goto string theory [80].

Therefore, in this paper, we test a set of dark energy–dark matter interacting models with the purpose of enlightening the physical properties of dark matter. In fact, the interaction term between the two fluids behaves as an *effective pressure*

entering the energy conservation equation, and consequently affecting the dust picture of dark matter. Thus, evaluating the effective equation of state parameter for the dark matter, we can discriminate between cold, warm, and hot models.

From the technical point of view, we employ Gaussian Process techniques for reconstructing the redshift evolution of the Hubble function with the purpose of selecting the best cosmological model involving energy flows between dark matter and dark energy. The latter is modeled in the form of the modified Chaplygin gas. In particular, we use 30 data points for $H = H(z)$ consisting of samples deduced from the differential age method, allowing the Gaussian Process to constrain the model parameters. Our purpose is to extend and complement the analysis of [81,82] by allowing a redshift-dependent equation of state for dark energy (for accounting for Planck observations), and interactions in the dark sector (for alleviating the coincidence problem).

Our paper is organized as follows: we introduce our cosmological model in Sect. 2 reviewing the physical properties of the modified Chaplygin gas and the features of the postulated energy exchanges between the two cosmic fluids. Then, in Sect. 3 we explain the importance of the cosmic chronometers as model-independent observational data for the reconstruction of the Hubble function, and for constraining the values of the free parameters entering our class of models. In sect. 4 we present the reconstruction for the Hubble function through gaussian processes, while in Sect. 5 we describe the numerical method we have adopted for the integration of the field equations. The same Sect. exhibits explicitly also our cosmological results comparing and contrasting between the different possible choices of the interaction term. Lastly, we conclude in Sect. 6 with some remarks about the importance of our study in light of the current literature estimates of the cosmological parameters by means of various different datasets.

2 Overview of the cosmological model

In this section we will introduce the basic equations of the cosmological model under investigation. For the geometrical modeling of the Universe we adopt the flat Friedmann metric which, in a Cartesian system of coordinates, reads [83]:

$$ds^2 = -dt^2 + a^2(t)(dx^2 + dy^2 + dz^2), \tag{1}$$

where $a(t)$ is the time-dependent scale factor of the Universe. Moreover, we picture the matter content of the Universe as two perfect fluids with energy density $\rho(t)$ and pressure $p(t)$, respectively. Their stress-energy tensors are $T^\mu_{\ \nu} = \text{diag}[-\rho_i(t), p_i(t), p_i(t), p_i(t)]$ with $i = de, m$ for dark energy and dark matter respectively. The relevant Ein-

stein field equation $G_{\mu\nu} = 8\pi G\, T_{\mu\nu}$ is given by

$$\left(\frac{\dot{a}}{a}\right)^2 := H^2 = \frac{1}{3M_p^2}\left[\rho_{de} + \rho_m\right], \tag{2}$$

where $M_p^2 = (8\pi G)^{-1}$ is the reduced Planck mass, H is the Hubble function, and an overdot denotes a time derivative. Then, the Bianchi identities $T^{\mu\nu}{}_{;\nu} = 0$ deliver

$$\dot{\rho}_m + 3H\rho_m = 0,$$
$$\dot{\rho}_{de} + 3H\left(\rho_{de} + p\right) = 0, \tag{3}$$

which account for two separately-conserved dark matter and dark energy fluids. However, in this paper we will introduce an interaction term Q between these two fluids breaking the Bianchi symmetry (of course the total energy of the Universe is still conserved because dark matter is transformed into dark energy or viceversa), and the coupled evolution of the two fluids is now given by

$$\dot{\rho}_m + 3H\rho_m = Q,$$
$$\dot{\rho}_{de} + 3H\left(\rho_{de} + p\right) = -Q. \tag{4}$$

2.1 Modeling of dark energy as a modified Chaplygin gas

For the modeling of the dark energy fluid we adopt the modified Chaplygin gas proposal based on the equation of state [84]:

$$p = A\rho_{de} - \frac{B}{\rho_{de}^\alpha}, \tag{5}$$

in which A, B and α are constant parameters while ρ_{de} is the energy density of the fluid. The modified version of the Chaplygin gas is an extension of the generalized Chaplygin gas whose limit corresponds to the choices $A = 0$ and $\alpha > 0$; also, selecting $A = 0$ and $\alpha = 1$ the model reduces to the original Chaplygin gas. The modified Chaplygin gas implements a form of *effective freedom* in the cosmic fluid [78,79]. In fact, if $\alpha > 0$ then the equation of state (5) reduces to that of an ideal fluid with pressure and energy density directly proportional to each other $p \propto \rho$ at high energies (which can possibly occur in the first instants after the big bang). On the other hand, if $\alpha < 0$ the linear behavior is realized at low energies (i.e., at late ages) when the fluid dilutes due to the expansion of the Universe. Since the constituents of an ideal gas have only kinetic and not potential energy, in these two regimes they essentially behave as free particles. The occurrence of one of these two cases will be explored in this paper through the use of the cosmic chronometers. The modified Chaplygin gas has been tested in [85–88] against Constitution+CMB+BAO data, and against Union+CMB+BAO observations using Markov Chain Monte Carlo techniques. In this paper, we will quantify the role of the interaction terms on the estimates of the cosmological parameters comparing with these literature results. More formally, exploiting the fluid–scalar field correspondence in the canonical framework [89,90], the pressure and energy density of the Chaplygin gas (5) can be related to the kinetic energy $X = -\frac{1}{2}g^{\mu\nu}\partial_\mu\phi\partial_\nu\phi$ and the potential V of a scalar field ϕ via:

$$\rho_{de} = \frac{\dot{\phi}^2}{2} + V, \quad p = \frac{\dot{\phi}^2}{2} - V, \tag{6}$$

or equivalently

$$V = \frac{1}{2}\left[(1-A)\rho_{de} + \frac{B}{\rho_{de}^\alpha}\right], \quad \dot{\phi}^2 = (1+A)\rho_{de} - \frac{B}{\rho_{de}^\alpha}. \tag{7}$$

Debnath et al. [91] has extensively investigated the characteristics of the potential $V = V(\phi)$ in a flat Friedmann Universe dominated by the modified Chaplygin gas. At early times, which correspond to $a(t) \to 0$ the potential can either approach zero (for $A = 1$), or diverge (for $A \neq 1$). At late times, which correspond to $a(t) \to \infty$, the potential approaches the constant value $V(\phi) \to \left(\frac{B}{1+A}\right)^{\frac{1}{1+\alpha}}$. Therefore, at late times for $A = -1$ the potential diverges if $\alpha > -1$, and approaches zero otherwise. Analytically, in a flat Friedmann universe whose only energy-matter content is the modified Chaplygin gas (5) the potential of the underlying self-interacting scalar field is [91,92]:

$$V(\phi) = \frac{1-A}{2}\left(\frac{B}{1+A}\right)^{\frac{1}{1+\alpha}}\cosh^{\frac{2}{1+\alpha}}\frac{\sqrt{3(1+A)}(1+\alpha)\phi}{2}$$
$$+ \frac{B}{2}\left(\frac{B}{1+A}\right)^{-\frac{\alpha}{1+\alpha}}\cosh^{-\frac{2}{1+\alpha}}\frac{\sqrt{3(1+A)}(1+\alpha)\phi}{2}. \tag{8}$$

2.2 Modeling of the interaction terms

An interaction term between the dark matter particles and the dark energy molecules behaves phenomenologically as an effective pressure Π which couples the conservation equations of the two cosmic fluids (breaking the Bianchi identities). In general, the interaction term would be written as [93,94]

$$Q = 3H\Pi. \tag{9}$$

In this paper, we consider an effective pressure parametrized as

$$\Pi = b \frac{\rho_{de}^m r^{-n} + (-1)^s \rho_m^m r^n}{\rho^u},$$ (10)

where the parameter b quantifies the strength of interactions between dark energy and dark matter. This quantity cannot be fixed by any theoretical first principle argument, and therefore its value will be estimated through the model selection procedure. A non-zero value for b can be interpreted as a manifestation of a fifth force mediated by a postulated *cosmon field* acting between dark matter and dark energy [95] violating the weak equivalence principle [96]. In particular, a positive b implies that dark energy is decaying into dark matter, while a negative sign is consistent with an energy flow in the opposite direction. The Le Châtelier–Braun principle favors a decay of dark energy into dark matter (and not viceversa) for maintaining the whole system close to thermal equilibrium because in this case the entropy of the universe will increase [97]. Interestingly, it seems that it is still an open question how to reconcile thermodynamically viable interacting models with the problem of formation of astrophysical structures [98]. In (10) $\rho = \rho_{de} + \rho_m$ is the total energy budget of the universe, and

$$r = \frac{\rho_{de}}{\rho_m}$$ (11)

is the relative abundance of the two cosmic fluids. In this section, we will show that the elegant parametrization (10) is rich enough for covering both the models with linear and nonlinear energy interactions, and with fixed or variable direction of the energy flow. In fact, for s odd the effective pressure Π is allowed, at least in principle, to switch its sign during the time evolution of the Universe depending on the interplay between the densities of the two dark fluids. This scenario would correspond to a phase transition between decelerating-accelerating (or viceversa) phases of the universe [99–101]. In light of this dependence on the background energy density when s is odd, the effective pressure can be interpreted as a *chameleon field* [76,77]. We stress that the interaction term (10) relies only on the abundance of the two dark fluids, and not on their physical nature or modeling (we just need to assume a time-evolving dark energy, which therefore rules out the case of a cosmological constant) [102]. To summarize, we can speak of *effective pressure* because in this class of models dark matter is behaving as a non-ideal fluid with equation of state parameter Π/ρ_m, and not any longer as pressureless dust [103]. The inferred value for the effective dark matter equation of state parameter will allow us to discriminate between the models of cold vs. warm vs. hot dark matter. The explicit models we will test in this paper

are:

$$Q_1 = 3Hb\rho_{de},$$ (12)

which corresponds to the choice $m = 1$, $n = 0$, $s \to \infty$, $u = 0$.

$$Q_2 = 3Hb\rho_m,$$ (13)

which corresponds to the choice $m = 1$, $n = 1$, $s \to \infty$, $u = 0$.

$$Q_3 = 3Hb(\rho_{de} + \rho_m),$$ (14)

which corresponds to the choice $m = 1, n = 0, s = 0, u = 0$.

$$Q_4 = 3Hb(\rho_{de} - \rho_m),$$ (15)

which corresponds to the choice $m = 1$, $n = 0$, $s = 1$, $u = 0$. In this model the effective pressure Π may switch its sign during the evolution of the universe depending on the relative abundance between the two dark fluids, inverting the direction of the energy flow from dark matter to dark energy.

$$Q_5 = 3Hb\sqrt{\rho_{de}\rho_m},$$ (16)

which corresponds to the choice $m = 1/2, n = 1/2, s \to \infty$, $u = 0$.

$$Q_6 = 3Hb\frac{\rho_{de}\rho_m}{\rho_{de} + \rho_m},$$ (17)

which corresponds to the choice $m = 2$, $n = 1$, $s \to \infty$, $u = 1$.

$$Q_7 = 3Hb\frac{\rho_{de}^2}{\rho_{de} + \rho_m},$$ (18)

which corresponds to the choice $m = 2$, $n = 0$, $s \to \infty$, $u = 1$.

$$Q_8 = 3Hb\frac{\rho_m^2}{\rho_{de} + \rho_m},$$ (19)

which corresponds to the choice $m = 2$, $n = 2$, $s \to \infty$, $u = 1$.

The interaction terms Q_3 and Q_4 are symmetric under the reflection $\rho_{de} \leftrightarrow \rho_m$. The linear interaction terms $Q_1 - Q_4$ can be interpreted as a first-order Taylor expansion, which holds at low energy densities for any parameterization of the term Q. On the other hand, an analogy with chemical and nuclear reactions suggests that the interaction term should depend on the product of the abundances of the two species

[104]. Lastly, looking at the Friedmann equation (2), we note that, as for any model with interactions, the evolution of the Hubble function remains decoupled from the evolution of the cosmic fluids [105]. We stress that when assuming these types of interactions, the following hypothesis should be made: interactions are negligible at high redshifts growing in strength at lower redshifts, motivating the analysis of their impact on the cosmological parameters from available observational datasets.

3 Cosmic chronometers data

The role of passively evolving early galaxies as *cosmic chronometers* permits to measure the expansion history of the Universe directly without the need of relying on any cosmological model, and in particular without the need of making any at *a priori* hypothesis on the nature of dark energy and dark matter. In fact, this approach is based on the measurement of the differential age evolution as a function of the redshift for these galaxies, which in turn provides a direct estimate of the Hubble parameter:

$$H(z) = -\frac{1}{(1+z)}\frac{dz}{dt} \approx -\frac{1}{(1+z)}\frac{\Delta z}{\Delta t}. \quad (20)$$

The redshift is related to the scale factor of the Universe via

$$1 + z = \frac{1}{a}. \quad (21)$$

The dependence on the measurement of a differential quantity, that is $\Delta z/\Delta t$, is the most important strength of this approach because it provides many advantages in minimizing some common sources of uncertainty and systematic effects (for a detailed discussion see [106]). We exploit 30 data points of $H = H(z)$ consisting of 30 point samples deduced from the differential age method. Keeping this in mind, first, we will use Gaussian Process techniques for reconstructing the Hubble vs. Redshift evolution, and then we will optimize the free parameters of our family of cosmological interacting models. The data points we will consider are taken from [107] and are exhibited in Table 1. Then, we can select the best model by estimating the differential area $\Delta A'$ as explained in detail in the next section.

4 Gaussian process techniques for the $H = H(z)$ reconstruction

Gaussian process techniques, which have been studied in detail in [108], constitute a set of model-independent algorithms that can be exploited for the reconstruction of the Hubble parameter; they are particularly useful when studying dark energy–dark matter interacting models. This procedure relies on the following assumptions. First, it is assumed that each observational datum satisfies a Gaussian distribution in such a way that the full set of observational data obey to a multivariate normal distribution. The relationship between two different data points is accounted for by a function called *covariance function*. The values of the data at some redshift point at which they have not been directly measured would be extrapolated with the use of the covariance function because the points obey to the multivariate normal distribution. Besides, also the derivative (up to some order) of the function, that we want to reconstruct, at these data points, can be calculated through the covariance function. Therefore, this mathematical formalism allows us to numerically reconstruct every smooth function at any point via its dependence on the data and the values of the slopes at those points. Thus, the crucial task in Gaussian process techniques is to determine the covariance function at different points starting from the available measured data.

In general, when reconstructing a mathematical function through a gaussian process algorithm, different functional behavior of the covariance function may be implemented. The most convenient choice is to consider the probability distribution of the measured data points keeping in mind that the Gaussian process should be regarded as a generalization of the Gaussian probability distribution. In this paper, the observational data are the distances D to the host galaxies which obey to a Gaussian distribution with certain known mean and variance. With this information in hand, Gaussian processes allow us to reconstruct at posteriorly the distribution of the function $H(z)$ implementing the known Gaussian distribution characterizing D into (20).

Therefore, the key of this algorithm is the covariance function $k(z_1, z_2)$ which correlates the values of the distance to a certain galaxy $D(z)$ at the two different redshift ages z_1 and z_2. In general, one can choose from different functional behaviors for the covariance function $k(z_1, z_2)$, all of which are characterized by the two hyperparameters σ_f and ℓ; the latter would be determined testing against the observational data via a marginal likelihood. As a subsequent step, exploiting the inferred covariance function, the values of the function we want to reconstruct can be extrapolated at any arbitrary redshift point for which no measured data are available. Then, using the relation between the Hubble function $H(z)$ and the distance D, the redshift evolution of the Hubble function can be provided. Due to its model independence, this method has been widely applied in the reconstruction of dark energy equation of state and of the Hubble parameter [109–112], or in the test of the concordance model [113–115], for the analysis of the dynamical features of the dark energy by taming the matter degeneracy [99], and in light of cosmic chronometers in the ΛCDM model [81]. The purpose of the present work is exactly to revisit the latter by considering an

Table 1 The observational data for $H = H(z)$ and their uncertainty σ_H in units of km/s/Mpc. The 30 data points were obtained from the differential age method of cosmic chronometers. This table is taken from [107] (see references therein for comments about each data point)

z	$H(z)$	σ_H	z	$H(z)$	σ_H
0.07	69	19.6	0.4783	80.9	9
0.09	69	12	0.48	97	62
0.12	68.6	26.2	0.593	104	13
0.17	83	8	0.68	92	8
0.179	75	4	0.781	105	12
0.199	75	5	0.875	125	17
0.2	72.9	29.6	0.88	90	40
0.27	77	14	0.9	117	23
0.28	88.8	36.6	1.037	154	20
0.352	83	14	1.3	168	17
0.3802	83	13.5	1.363	160	33.6
0.4	95	17	1.4307	177	18
0.4004	77	10.2	1.53	140	14
0.4247	87.1	11.1	1.75	202	40
0.44497	92.8	12.9	1.965	186.5	50.4

evolving dark energy equation of state based on the modified Chaplygin gas fluid.

In this paper we adopt a gaussian exponential distribution as our covariance function $k(z_1, z_2)$:

$$k(z_1, z_2) = \sigma_f^2 \exp\left(-\frac{(z_1 - z_2)^2}{2\ell^2}\right). \tag{22}$$

We can reconstruct the redshift evolution of the Hubble function and that of the equation of state of dark energy (modified Chaplygin gas in our case) by modifying the *GaPP* package developed in [108]. We exhibit the outcome of the Reconstruction Process in Fig. 1 in which we display both the reconstructed H vs. z curve and the 30 model-independent measurements of $H(z)$ with the corresponding error bars we have used (compare with Table 1). The blue surface represents the 1σ confidence region of the reconstruction.

Fig. 1 The figure displays the reconstructed curve for $H = H(z)$ using Gaussian process techniques assuming an exponential covariance function and the 30 model-independent measurements of $H(z)$ with the corresponding error bars. The blue surface represents the 1σ confidence region of the reconstruction

5 Numerical analysis

We integrate the system constituted by the Friedmann equation (2) and by the energy conservation equations (4) using the iterative numerical differential equations solvers known under the name of *Runge–Kutta method* [116]. This method uses the input for the initial values, let us say (x_n, y_n), for evolving them into (x_{n+1}, y_{n+1}) by use of a discretized system of equations. Explicitly, the steps of the numerical algorithm we used to integrate our system of differential equations read as [116]:
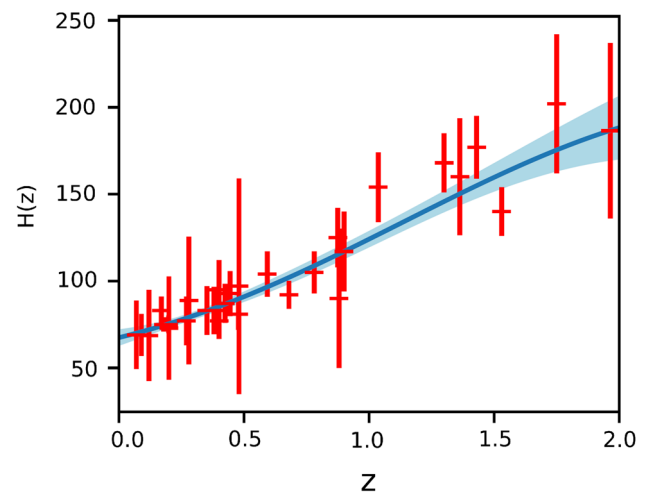
$$
\begin{aligned}
K1 &= h \cdot f(x_n, y_n), \\
K_2 &= h \cdot f\left(x_n + \frac{h}{2}, y_n + \frac{K_1}{2}\right), \\
K_3 &= h \cdot f\left(x_n + \frac{h}{2}, y_n + \frac{K_2}{2}\right), \\
K_4 &= h \cdot f(x_n + h, y_n + K_3), \\
y_{n+1} &= y_n + \frac{K_1}{6} + \frac{K_2}{3} + \frac{K_3}{3} + \frac{K_4}{6},
\end{aligned}
\tag{23}
$$

where h is the step size and $f(x, y)$ is the differential equation to solve, i.e. the Friedmann equation and energy conservation equations, respectively. Once provided with a set of initial conditions, this algorithm is able to deliver the values for the Hubble function, the energy density of dark matter and of dark energy for each interacting model. After integrating numerically the theoretical field equations, we implement the procedures from [111] for the gaussian reconstruction, and from [81] for the model selection:

- We use the data from Table 1 to generate the mock samples for the 30 values of the Hubble function at the same redshift, and for each redshift value $z_i (i = 1, \ldots, 30)$, assuming that the measurements follow a Gaussian randomized distribution:

$$H^{\text{mock}}(z_i) = H(z_i) + r\sigma_i, \qquad (24)$$

where r is a Gaussian random variable with mean 0, variance 1, and σ_i is the dispersion at z_i.

- Then, we reconstruct the mock function $H^{mock}(z)$, and we calculate a normalized absolute area difference between this function and the actual function using the formula

$$\Delta A' = \frac{\int_0^2 dz \left| H^{\text{mock}}(z) - H(z) \right|}{\int_0^2 dz H(z)}. \qquad (25)$$

The probability that the theoretical prediction of our cosmological model differs from the reconstructed function is quantified by the differential area $\Delta A'$ which should be minimized by optimizing appropriately the values of the model free parameters. In fact, we will need to estimate the possible randomized realizations which come with a differential area smaller than a specific value by presenting the cumulative probability distribution versus $\Delta A'$. In our paper we are required to adopt this so-called *Area Minimization Statistic* rather than discrete sampling statistics, e.g. weighted least squares, because we are comparing two continuous curves and not isolated points [117, Sect.5].

- Lastly, we build the distribution of frequency versus differential area $\Delta A'$ from which we can construct the cumulative probability distribution.

Applying this procedure to every interacting model Q_i that we have introduced in Sect. 2, we calculate the differential area $\Delta A'$ from (25) by replacing H_{mock} with the reconstructed function $H_i(z)$. Furthermore, we optimize the values of the free parameters characterizing each model (three parameters (A, B, α) which enter the equation of state of the modified Chaplygin gas as from (5), and the parameter b quantifying the strength of the interactions between

dark energy and dark matter). We allow these free parameters to take values in the following ranges: $H_0 \in (40, 90)$, $\Omega_{m0} \in (0.2, 0.7)$, A $\in (-2, 2)$, B $\in (-2, 2)$, b $\in (-1, 1)$, and $\alpha \in (-1.0, 1.0)$.

5.1 Numerical results

Being the cosmic chronometers data in Table 1 dependent on the redshift and not on the time, for tackling the optimization process it is mathematically convenient to recast the model equations (2)–(4)–(5) as

$$\frac{dH}{dz} = \frac{3H^2 + p}{2(1+z)H}, \quad \frac{d\Omega_m}{dz} = -\frac{Q + 3H\Omega_m p}{3(1+z)H^3},$$

$$p = 3A(1 - \Omega_m)H^2 - \frac{B}{(3(1 - \Omega_m)H^2)^\alpha}, \qquad (26)$$

where we have used (20), the definitions of the matter parameters $\Omega_{de} = \frac{\rho_{de}}{3H^2}$ and $\Omega_m = \frac{\rho_m}{3H^2}$, and the Friedman equation $\Omega_{de} + \Omega_m = 1$. Each interaction term Q_i should also be re-expressed as a function of Ω_m and H^2, rather than of ρ_m and ρ_{de}, accordingly.

We exhibit in Table 2 the best fit values for the model parameters H_0, Ω_{m0}, A, B, α, and b for each dark energy–dark matter interacting model. Table 3 shows the present-day values of the deceleration parameter q_0, adiabatic speed of sound squared for the dark energy fluid $c_s^2 = \frac{\partial p}{\partial \rho_{de}} = A + \frac{\alpha B}{\rho_{de}^{\alpha+1}}$, and the effective equation of state parameters for dark energy $\omega = \frac{p}{\rho_{de}}$, and dark matter $\omega_{eff} = \frac{\Pi}{\rho_m}$ for each interacting model. The deceleration parameter is computed using the formula $q = \frac{1 + 3\omega(1-\Omega_m)}{2}$. We display in Fig. 2 the cumulative distribution of the differential area $\Delta A'$, as calculated from (25), for each cosmological model under investigation. We remind that the interaction terms between dark energy and dark matter can be found in (12), $\ldots$, (19) for $Q_1, \ldots, Q_8$ respectively and that the former fluid is pictured according to the equation of state (5).

The error bars presented in Table 2 are found by applying Markov-Chain-Monte-Carlo hammer (emcee) Bayesian data analysis with flat priors about the mean values we have previously found through the interplay of gaussian reconstruction and optimization process[1] [118]. This procedure relies on the assumption that the data in Table 1 come with independent Gaussian errors, and we refer to [119] for an assessment of this claim. Then, the error bars in Table 3 are computed from those in Table 2 via the propagation formula

---

[1] Our python code is an appropriate re-elaboration of the freely available one https://emcee.readthedocs.io/en/stable/tutorials/line/.

$$\sigma_{f(x,y,z,...)}$$

$$= \sqrt{\left(\frac{\partial f(x,y,z,\ldots)}{\partial x}\right)^2 \sigma_x^2 + \left(\frac{\partial f(x,y,z,\ldots)}{\partial y}\right)^2 \sigma_y^2 + \left(\frac{\partial f(x,y,z,\ldots)}{\partial z}\right)^2 \sigma_z^2 + \cdots.} \tag{27}$$

Moreover, we have found that should we replace the gaussian kernel (22) with the Matérn one[2] [81, Eq.(A.1)]

$$k(z_1, z_2) = \sigma_f^2 \exp\left(-\frac{3|z_1 - z_2|}{l}\right)$$

$$\times \left(1 + \frac{3|z_1 - z_2|}{l} + \frac{27|z_1 - z_2|^2}{7l^2}\right.$$

$$\left. + \frac{18|z_1 - z_2|^3}{7l^3} + \frac{27|z_1 - z_2|^4}{35l^4}\right) \tag{28}$$

in the reconstruction of the cosmic history $H = H(z)$ before performing the optimization process, the estimates of the mean values we have presented in Table 2 would be affected at most by a 3% variation. This is less than both their 1σ uncertainty and than the uncertainties which affect the astrophysical data from Table 1 on which the reconstruction is based.

5.2 Discussion

First of all, it should be noted that the results exhibited in Table 2 clearly suggest that the simplest one-parameter Chaplygin gas model $p = -\frac{B}{\rho_{de}}$ cannot account for the cosmic chronometers data because we have obtained that the dark energy density should come with a positive power, e.g. $\alpha < 0$, in its equation of state. More technically, when insisting to assume such a model, we could not find any global minimum for the differential area $\Delta A'$ when performing the optimization process. This result should not be naively interpreted as suggesting that a three-parameter model like the modified Chaplygin gas of (5) performs better than the Chaplygin gas just because it involves two more free parameters which can be appropriately tuned, but it is a genuinely physical result. We would like to mention as well that this is not the first time that a negative value of α is estimated: see for example [120,121] where Planck 2015, type-Ia supernovae, and Hubble parameter data are used. In this paper we found that assuming the dark sector to be composed by two components interacting with each other, our estimates deviate more from the Chaplygin gas

behavior than the ones in this previous investigation. Furthermore, it should be noted also that the scenario in which no energy flows between dark energy and dark matter occur is not favoured either, and that the best model is actually the one based on non-linear interactions between dark matter and dark energy as $\sim \rho_m^2/(\rho_m + \rho_{de})$. More specifically, the optimization process applied to the ΛCDM model delivers the estimates $H_0 = 70.17^{+2.88}_{-2.75}$, $\Omega_{m0} = 0.2844^{+0.1001}_{-0.0991}$, $q_0 = -0.3279^{+0.1042}_{-0.1051}$, with $\Delta A' = 0.02249$; it should be noted that already the results reported in Table 2 implicitly suggest that according to our analysis ΛCDM is not the favoured model because it can be obtained from ours by fixing $A = -1$, $B = 0 = b$. We need also to remark that the estimates of the cosmological parameters for all the modelings of the interaction terms presented in Tables 2 and 3 are degenerate with each other within the 1σ interval.

A more transparent physical characterization of the dark energy fluid modeled according to the modified Chaplygin gas (5) comes from the study of the following energy conditions [122]:

Null energy condition: $\rho + p \geq 0;$ (29)

Weak energy condition: $\rho \geq 0, \quad \rho + p \geq 0;$ (30)

Dominant energy condition: $\rho \geq |p|;$ (31)

Strong energy condition: $\rho + p \geq 0, \quad \rho + 3p \geq 0.$ (32)

Explicitly they read as:

Null energy condition: $(1+A)\rho - \frac{B}{\rho^\alpha} \geq 0;$ (33)

Weak energy condition: $\rho \geq 0, \quad (1+A)\rho - \frac{B}{\rho^\alpha} \geq 0;$ (34)

Dominant energy condition: $\rho \geq \left| A\rho - \frac{B}{\rho^\alpha} \right|;$ (35)

Strong energy condition: $(1+A)\rho - \frac{B}{\rho^\alpha} \geq 0, \quad (1+3A)\rho - \frac{3B}{\rho^\alpha} \geq 0.$ (36)

For example, a phantom energy fluid violates all the null, weak, and strong energy conditions [123–128], while a cosmological constant term and a quintessence fluid violate only the strong energy condition [129–131]. For the case of the modified Chaplygin gas analyzed in this paper, considering the present-day value of the effective equation of state parameter ω from Table 3, we can conclude that regardless the

---

[2] It is already known that the Matérn kernel provides a less smooth reconstructed curve for the function $H(z)$ vs. z [81, Fig.7] making more problematic for the ΛCDM model to account for the data at high redshift because the reconstruction delivers a slower increase than the one predicted by the model.

Table 2 The optimal values for the model free parameters A, B, α, b, H_0 and Ω_{m0} for each dark energy–dark matter interacting model. We remind that the equation of state we are adopting for the dark energy is $p = A\rho_{de} - \frac{B}{\rho_{de}^\alpha}$, and that b quantifies the strength of interaction between dark energy and dark matter according to the modelings (12), ..., (19) for $Q_1, \ldots, Q_8$ respectively. For the case of Q_0 appearing in the last row we have set $b = 0$, i.e. no interaction between dark energy and dark matter, by assumption. The best models in light of cosmic chronometers data are the ones with a lower value of $\Delta A'$. The Hubble constant is expressed in units of km/Mpc/s

| Q_i | Parameters | | | | | | |
	$\Delta A'$	H_0	Ω_{m0}	A	B	α	b
Q_1	0.01306	$66.48^{+9.97}_{-10.09}$	$0.3107^{+0.0994}_{-0.0987}$	$-0.3343^{+0.1004}_{-0.0988}$	$1.8493^{+0.1001}_{-0.0991}$	$-0.8334^{+0.0099}_{-0.0099}$	$0.0830^{+0.0993}_{-0.1008}$
Q_2	0.01220	$66.47^{+9.88}_{-9.89}$	$0.3145^{+0.1002}_{-0.1004}$	$-0.0002^{+0.1009}_{-0.0999}$	$1.6758^{+0.1007}_{-0.0991}$	$-0.9168^{+0.0099}_{-0.0097}$	$0.0837^{+0.0993}_{-0.1004}$
Q_3	0.02023	$66.52^{+9.90}_{-10.00}$	$0.4580^{+0.0990}_{-0.0988}$	$-0.1951^{+0.0993}_{-0.1004}$	$2.1950^{+0.1000}_{-0.0989}$	$-0.9100^{+0.0098}_{-0.0096}$	$0.0827^{+0.0980}_{-0.1007}$
Q_4	0.01733	$66.55^{+10.07}_{-9.92}$	$0.2961^{+0.1004}_{-0.0992}$	$-0.5401^{+0.0990}_{-0.0999}$	$2.4000^{+0.0993}_{-0.0085}$	$-0.7500^{+0.0099}_{-0.0097}$	$0.0854^{+0.0986}_{-0.0996}$
Q_5	0.01269	$66.44^{+10.02}_{-9.82}$	$0.3147^{+0.0990}_{-0.1001}$	$-0.3332^{+0.0989}_{-0.1000}$	$2.0252^{+0.0996}_{-0.0993}$	$-0.8333^{+0.0099}_{-0.0100}$	$0.0836^{+0.0988}_{-0.0989}$
Q_6	0.01275	$66.47^{+10.04}_{-9.90}$	$0.3159^{+0.0992}_{-0.0997}$	$-0.3332^{+0.0993}_{-0.0996}$	$2.0246^{+0.0996}_{-0.0994}$	$-0.8334^{+0.0100}_{-0.0098}$	$0.1670^{+0.0999}_{-0.0995}$
Q_7	0.01383	$66.44^{+9.92}_{-9.96}$	$0.3143^{+0.0996}_{-0.1002}$	$-0.5001^{+0.0993}_{-0.0985}$	$2.0252^{+0.0992}_{-0.0997}$	$-0.7501^{+0.0099}_{-0.0099}$	$0.1669^{+0.0984}_{-0.0994}$
Q_8	0.01168	$66.51^{+9.93}_{-9.83}$	$0.3146^{+0.0994}_{-0.0995}$	$-0.1669^{+0.0992}_{-0.0982}$	$1.3250^{+0.0997}_{-0.0994}$	$-0.9166^{+0.0099}_{-0.0100}$	$0.1673^{+0.0985}_{-0.0999}$
Q_0	0.02157	$66.54^{+9.85}_{-9.92}$	$0.3188^{+0.0988}_{-0.0975}$	$-0.5997^{+0.0995}_{-0.1003}$	$1.4409^{+0.0984}_{-0.0995}$	$-0.0808^{+0.0987}_{-0.0983}$	0

Table 3 The present-day values of the deceleration parameter q_0, adiabatic speed of sound squared for the dark energy fluid $c_s^2 = \frac{\partial p}{\partial \rho_{de}}$, and the effective equation of state parameters for dark energy $\omega = \frac{p}{\rho_{de}}$ and dark matter $\omega_{eff} = \frac{\Pi}{\rho_m}$ for each cosmological model. These quantities have been computed from those in Table 2 and the corresponding error bars are found by applying the propagating formula (27). The expressions for the interaction terms $Q_1, \ldots, Q_8$ can be found in (12), ..., (19) respectively. The model Q_0 corresponds to the choice $b = 0$, i.e. no interaction between dark energy and dark matter. The best model in light of the cosmic chronometers data is Q_8 (see Table 2). The uncertainties are hugely affected by the errors on the datapoints at high redshift $z \sim 2$ and on the datapoint at $z = 0.48$ (see Table 1). A complete discussion on the cosmological consequences of the results here presented can be found in Sect. 5.2

Q_i	q_0	c_s^2	ω	ω_{eff}
Q_1	$-0.2640^{+0.1127}_{-0.1112}$	$-0.6715^{+0.1077}_{-0.1061}$	$-0.7389^{+0.1090}_{-0.1075}$	$0.1841^{+0.2203}_{-0.2236}$
Q_2	$-0.3074^{+0.1357}_{-0.1338}$	$-0.7199^{+0.1316}_{-0.1298}$	$-0.785^{+0.1319}_{-0.1302}$	$0.0836^{+0.0993}_{-0.1004}$
Q_3	$-0.4444^{+0.1128}_{-0.1124}$	$-1.0747^{+0.1387}_{-0.1382}$	$-1.1617^{+0.1387}_{-0.1448}$	$0.1805^{+0.2139}_{-0.2198}$
Q_4	$-0.3279^{+0.1042}_{-0.1051}$	$-0.7230^{+0.1007}_{-0.1016}$	$-0.7840^{+0.1014}_{-0.1023}$	$0.1176^{+0.1164}_{-0.1160}$
Q_5	$-0.2981^{+0.1119}_{-0.1130}$	$-0.7025^{+0.1073}_{-0.1085}$	$-0.7764^{+0.1088}_{-0.1100}$	$0.1233^{+0.1457}_{-0.1459}$
Q_6	$-0.2971^{+0.1122}_{-0.1122}$	$-0.7029^{+0.1079}_{-0.1079}$	$-0.7768^{+0.1094}_{-0.1093}$	$0.1142^{+0.0683}_{-0.0680}$
Q_7	$-0.2279^{+0.1044}_{-0.1036}$	$-0.6558^{+0.1008}_{-0.1001}$	$-0.7077^{+0.1015}_{-0.1007}$	$0.2496^{+0.1472}_{-0.1487}$
Q_8	$-0.3085^{+0.1264}_{-0.1258}$	$-0.7347^{+0.1223}_{-0.1217}$	$-0.7864^{+0.1230}_{-0.1224}$	$0.0526^{+0.0309}_{-0.0314}$
Q_0	$-0.1131^{+0.1016}_{-0.1024}$	$-0.5997^{+0.0995}_{-0.1003}$	$-0.6000^{+0.0995}_{-0.1003}$	0

modeling of the interaction term, but for Q_3, only the strong energy condition is violated. This is a remarkable difference between our class of interacting models versus the strengthened dark energy proposal of [132] which instead violates also the null and weak energy conditions.

Since our numerical investigation suggests that $c_s^2 < 0$, we need to mention that the issue of the stability under small-wavelength perturbations for such configurations was addressed in [89,133,134], and indeed literature exhibits examples of cosmological applications involving fluids supported by a negative adiabatic speed of sound squared [135].

Combined interpretation of the Planck Power Spectra + Baryon Acoustic Oscillation + Lens in a perturbed flat Friedmann Universe has allowed the reconstruction of the cosmic history of the dark matter equation of state [136] in the framework of so-called "Generalized Dark Matter" [136,137]. Our results exhibited in Table 3 show that cosmic chronometers data favor the coldest dark matter equation of state, that is, the one with the smallest deviation of the effective equation of state parameter from zero, although this does not mean the one with the weakest coupling b between the two dark fluids because of the non-linear form of the interaction term. In light of this analysis, the plausible candidates for dark matter should be objects with slower non-relativistic velocities. More in general, for all the possible dark energy–dark matter interactions that we have assumed we have obtained a
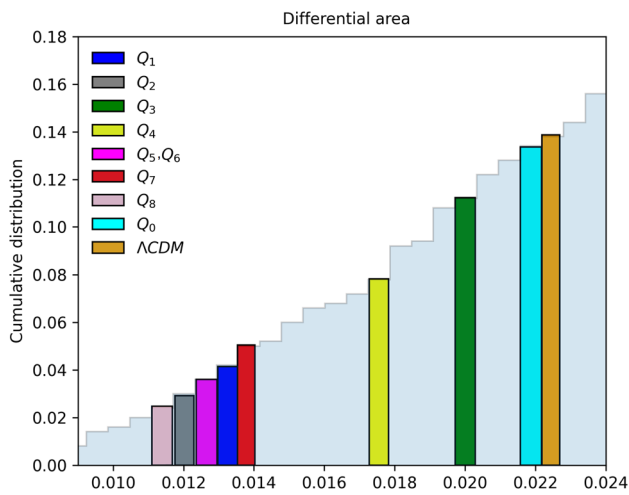
Fig. 2 This figure depicts the cumulative distribution of the differential area $\Delta A'$, as calculated from (25), and whose numerical results are reported in Table 2 together with the optimal values for the model free parameters. The specific forms of the dark energy–dark matter interaction terms $Q_1, \ldots, Q_8$ can be found in Eqs. (12), ..., (19) respectively. The notation Q_0 refers to the scenario in which no energy flow between the two components of the dark sector are assumed. A lower value of $\Delta A'$ indicates that the corresponding interaction term is favoured by the cosmic chronometers data. As a term of comparison we exhibit also the result for the ΛCDM model. The cosmological consequences of these results are explored in Table 3, where the corresponding values for the present day deceleration parameter, adiabatic speed of sound inside the dark energy fluid, and effective equation of state parameters for dark energy and dark matter are exhibited. We refer as well to Sect. 5.2 for a discussion about the cosmological meaning of our results

positive value for the parameter b implying that dark energy is decaying into the dark matter in agreement with the Le Châtelier–Braun principle [97].

6 Conclusion

In this paper, we have shown that also a model selection in light of the cosmic chronometer datasets favors some sort of interaction between dark energy and dark matter beyond the coincidence problem and the Hubble tension issue already extensively investigated in the literature. Another way of interpreting our result would be that in our framework dark matter is not any longer a pressure-less dust fluid but a material with a non-trivial evolving equation of state as in the "Generalized Dark Matter" proposal because the interaction term can be recast as an effective contribution to the dark matter pressure. In fact, the fitting procedure has delivered a nonzero value for the constant quantifying the amount of the energy flow between dark energy and dark matter. Our result seems quite robust because we have explored many possible different realizations of the interaction term beyond the first-order linear approximation by allowing it to depend on several combinations of the dark energy, or on the dark mat-

ter amount, or on a combination of them. Similarly, we have obtained estimates of $H_0 \simeq 66$ km/s/Mpc and $\Omega_m \simeq 0.3$ for all the interaction terms we have assumed. Furthermore, our analysis keeps suggesting that the simpler cosmological constant modeling of the dark energy fluid should be replaced by some sort of evolving field, and actually that also the generalized Chaplygin gas scenario (arising in the stringy Born–Infeld theory) should be promoted to the case of the modified Chaplygin gas. Moreover, we have also commented that an interaction term between the two cosmic fluids may also avoid the occurrence of a big rip singularity without the need of invoking any mysterious quantum gravity effect because a phantom fluid scenario was ruled out by investigating the energy conditions for the best-fit values of the model parameters. In a set of future works, we will explore more in detail whether our results depend on the particular fluid approach chosen for the modeling of the dark energy.

References

1. F. Iocco, M. Pato, G. Bertone, Evidence for dark matter in the inner Milky Way. Nat. Phys. **11**, 245 (2015). https://doi.org/10.1038/nphys3237. arXiv:1502.03821 [astro-ph.GA]
2. P.J.E. Peebles, *Principles of Physical Cosmology* (Princeton University Press, Princeton, 1993)
3. R.A. Battye, A. Moss, Evidence for massive neutrinos from cosmic microwave background and lensing observations. Phys. Rev. Lett. **112**(5), 051303 (2014). https://doi.org/10.1103/PhysRevLett.112.051303. arXiv:1308.5870 [astro-ph.CO]
4. S. Dodelson, L.M. Widrow, Sterile-neutrinos as dark matter. Phys. Rev. Lett. **72**, 17 (1994). https://doi.org/10.1103/PhysRevLett.72.17. arXiv:hep-ph/9303287

5. R.D. Peccei, The strong CP problem and axions. Lect. Notes Phys. **741**, 3 (2008). https://doi.org/10.1007/978-3-540-73518-2_1. arXiv:hep-ph/0607268

6. D. Hooper, L.T. Wang, Possible evidence for axino dark matter in the galactic bulge. Phys. Rev. D **70**, 063506 (2004). https://doi.org/10.1103/PhysRevD.70.063506. arXiv:hep-ph/0402220

7. F. Takayama, M. Yamaguchi, Gravitino dark matter without R-parity. Phys. Lett. B **485**, 388 (2000). https://doi.org/10.1016/S0370-2693(00)00726-7. arXiv:hep-ph/0005214

8. J. Ellis, K.A. Olive, Supersymmetric dark matter candidates, in Particle Dark Matter, ed. by G. Bertone, pp. 142–163. Hardback. ISBN 9780521763684. arXiv:1001.3651 [astro-ph.CO]

9. K.N. Abazajian, Detection of dark matter decay in the X-ray. arXiv:0903.2040 [astro-ph.CO]

10. G. Bertone et al., *Particle Dark Matter: Observations Models and Searches* (Cambridge University Press, Cambridge, 2010)

11. J.R. Bond, G. Efstathiou, J. Silk, Massive neutrinos and the large scale structure of the Universe. Phys. Rev. Lett. **45**, 1980 (1980). https://doi.org/10.1103/PhysRevLett.45.1980

12. U. Seljak, M. Zaldarriaga, Direct signature of an evolving gravitational potential from the cosmic microwave background. Phys. Rev. D **60**, 043504 (1999). https://doi.org/10.1103/PhysRevD.60.043504

13. S. Dodelson, L.M. Widrow, Sterile-neutrinos as dark matter. Phys. Rev. Lett. **72**, 17 (1994). https://doi.org/10.1103/PhysRevLett.72.17. arXiv:hep-ph/930328

14. R.D. Peccei, H.R. Quinn, Constraints imposed by CP conservation in the presence of pseudoparticles. Phys. Rev. D **16**, 1791 (1977). https://doi.org/10.1103/PhysRevD.16.1791

15. J. Polchinski, *String Theory. Vol. 2: Superstring Theory and Beyond* (Cambridge University Press, Cambridge, 1998)

16. P.A.R. Ade et al. (Planck Collaboration), Planck 2015 results. XIII. Cosmological parameters. Astron. Astrophys. **594**, A13 (2016). https://doi.org/10.1051/0004-6361/201525830. arXiv:1502.01589 [astro-ph.CO]

17. H.E.S. Velten, R.F. vom Marttens, W. Zimdahl, Aspects of the cosmological coincidence problem. Eur. Phys. J. C **74**(11), 3160 (2014). https://doi.org/10.1140/epjc/s10052-014-3160-4. arXiv:1410.2509 [astro-ph.CO]

18. G. Leon, E.N. Saridakis, Phantom dark energy with varying-mass dark matter particles: acceleration and cosmic coincidence problem. Phys. Lett. B **693**, 1–10 (2010). https://doi.org/10.1016/j.physletb.2010.08.016. arXiv:0904.1577 [gr-qc]

19. R. Cai, A. Wang, Cosmology with interaction between phantom dark energy and dark matter and the coincidence problem. JCAP **03**, 002 (2005). https://doi.org/10.1088/1475-7516/2005/03/002. arXiv:hep-th/0411025

20. N. Arkani-Hamed, L.J. Hall, C.F. Kolda, H. Murayama, A new perspective on cosmic coincidence problems. Phys. Rev. Lett. **85**, 4434–4437 (2000). https://doi.org/10.1103/PhysRevLett.85.4434. arXiv:astro-ph/0005111

21. S. Kumar, R.C. Nunes, Echo of interactions in the dark sector. Phys. Rev. D **96**, 103511 (2017). https://doi.org/10.1103/PhysRevD.96.103511. arXiv:1702.02143 [astro-ph.CO]

22. S. Kumar, R.C. Nunes, S.K. Yadav, Dark sector interaction: a remedy of the tensions between CMB and LSS data. Eur. Phys. J. C **79**, 576 (2019). https://doi.org/10.1140/epjc/s10052-019-7087-7. arXiv:1903.04865 [astro-ph.CO]

23. S. Kumar, R.C. Nunes, Probing the interaction between dark matter and dark energy in the presence of massive neutrinos. Phys. Rev. D **94**, 123511 (2016). https://doi.org/10.1103/PhysRevD.94.123511. arXiv:1608.02454 [astro-ph.CO]

24. W. Yang, S. Pan, R.C. Nunes, D.F. Mota, Dark calling dark: interaction in the dark sector in presence of neutrino properties after Planck CMB final release. JCAP **04**, 008 (2020). https://doi.org/10.1088/1475-7516/2020/04/008. arXiv:1910.08821 [astro-ph.CO]

25. E. Di Valentino, A. Melchiorri, O. Mena, Can interacting dark energy solve the H_0 tension? Phys. Rev. D **96**(4), 043503 (2017). https://doi.org/10.1103/PhysRevD.96.043503. arXiv:1704.08342 [astro-ph.CO]

26. E. Di Valentino, A. Melchiorri, O. Mena, S. Vagnozzi, Interacting dark energy after the latest Planck, DES, and H_0 measurements: an excellent solution to the H_0 and cosmic shear tensions. Phys. Dark Univ. **30**, 100666 (2020)

27. L. Amendola, G. Camargo Compos, R. Rosenfeld, Consequences of dark matter-dark energy interaction on cosmological parameters derived from SNIa data. Phys. Rev. D **75**, 083506 (2007). https://doi.org/10.1103/PhysRevD.75.083506. arXiv:astro-ph/0610806

28. J. He, B. Wang, Effects of the interaction between dark energy and dark matter on cosmological parameters. JCAP **06**, 010 (2008). https://doi.org/10.1088/1475-7516/2008/06/010. arXiv:0801.4233 [astro-ph]

29. E. Abdalla, L. Abramo, J.C. de Souza, Signature of the interaction between dark energy and dark matter in observations. Phys. Rev. D **82**, 023508 (2010). https://doi.org/10.1103/PhysRevD.82.023508. arXiv:0910.5236 [gr-qc]

30. L. Lopez Honorez, B.A. Reid, O. Mena, L. Verde, R. Jimenez, Coupled dark matter-dark energy in light of near Universe observations. JCAP **09**, 029 (2010). https://doi.org/10.1088/1475-7516/2010/09/029. arXiv:1006.0877 [astro-ph.CO]

31. T. Clemson, K. Koyama, G. Zhao, R. Maartens, J. Valiviita, Interacting dark energy—constraints and degeneracies. Phys. Rev. D **85**, 043007 (2012). https://doi.org/10.1103/PhysRevD.85.043007. arXiv:1109.6234 [astro-ph.CO]

32. S. Pan, S. Bhattacharya, S. Chakraborty, An analytic model for interacting dark energy and its observational constraints. Mon. Not. R. Astron. Soc. **452**(3), 3038 (2015). https://doi.org/10.1093/mnras/stv1495. arXiv:1210.0396 [gr-qc]

33. V. Salvatelli, A. Marchini, L. Lopez-Honorez, O. Mena, New constraints on coupled dark energy from the Planck satellite experiment. Phys. Rev. D **88**(2), 023531 (2013). https://doi.org/10.1103/PhysRevD.88.023531. arXiv:1304.7119 [astro-ph.CO]

34. S. Pan, S. Chakraborty, A cosmographic analysis of holographic dark energy models. Int. J. Mod. Phys. D **23**(11), 1450092 (2014). https://doi.org/10.1142/S0218271814500928. arXiv:1410.8281 [gr-qc]

35. E. Ferreira, G.M.J. Quintin, A.A. Costa, E. Abdalla, B. Wang, Evidence for interacting dark energy from BOSS. Phys. Rev. D **95**(4), 043520 (2017). https://doi.org/10.1103/PhysRevD.95.043520. arXiv:1412.2777 [astro-ph.CO]

36. R. Murgia, S. Gariazzo, N. Fornengo, Constraints on the coupling between dark energy and dark matter from CMB data. JCAP **04**, 014 (2016). https://doi.org/10.1088/1475-7516/2016/04/014. arXiv:1602.01765 [astro-ph.CO]

37. W. Yang, H. Li, Y. Wu, J. Lu, Cosmological constraints on coupled dark energy. JCAP **10**, 007 (2016). https://doi.org/10.1088/1475-7516/2016/10/007. arXiv:1608.07039 [astro-ph.CO]

38. S. Pan, G. Sharov, A model with interaction of dark components and recent observational data. Mon. Not. R. Astron. Soc. **472**(4), 4736 (2017). https://doi.org/10.1093/mnras/stx2278. arXiv:1609.02287 [gr-qc]

39. I. Odderskov, M. Baldi, L. Amendola, The effect of interacting dark energy on local measurements of the Hubble constant. JCAP **05**, 035 (2016). https://doi.org/10.1088/1475-7516/2016/05/035. arXiv:1510.04314 [astro-ph.CO]

40. R. von Marttens, L. Lombriser, M. Kunz, V. Marra, L. Casarini, J. Alcaniz, Dark degeneracy I: dynamical or interacting dark energy? Phys. Dark Univ. **28**, 100490 (2020). https://doi.org/10.1016/j.dark.2020.100490. arXiv:1911.02618 [astro-ph.CO]

41. J. Mifsud, C. Van De Bruck, Probing the imprints of generalized interacting dark energy on the growth of perturbations. JCAP **11**, 001 (2017). https://doi.org/10.1088/1475-7516/2017/11/001. arXiv:1707.07667 [astro-ph.CO]

42. J. Valiviita, E. Majerotto, R. Maartens, Instability in interacting dark energy and dark matter fluids. JCAP **07**, 020 (2008). https://doi.org/10.1088/1475-7516/2008/07/020. arXiv:0804.0232 [astro-ph]

43. G. Caldera-Cabral, R. Maartens, B.M. Schaefer, The growth of structure in interacting dark energy models. JCAP **07**, 027 (2009). https://doi.org/10.1088/1475-7516/2009/07/027. arXiv:0905.0492 [astro-ph.CO]

44. E. Majerotto, J. Valiviita, R. Maartens, Adiabatic initial conditions for perturbations in interacting dark energy models. Mon. Not. R. Astron. Soc. **402**, 2344–2354 (2010). https://doi.org/10.1111/j.1365-2966.2009.16140.x. arXiv:0907.4981 [astro-ph.CO]

45. F. Fontanot, M. Baldi, V. Springel, D. Bianchi, Semi-analytic galaxy formation in coupled dark energy cosmologies. Mon. Not. R. Astron. Soc. **452**(1), 978 (2015). https://doi.org/10.1093/mnras/stv1345. arXiv:1505.02770 [astro-ph.CO]

46. M. Baldi, Clarifying the effects of interacting dark energy on linear and nonlinear structure formation processes. Mon. Not. R. Astron. Soc. **414**, 116 (2011). https://doi.org/10.1111/j.1365-2966.2011.18263.x. arXiv:1012.0002 [astro-ph.CO]

47. B. Li, J.D. Barrow, On the effects of coupled scalar fields on structure formation. Mon. Not. R. Astron. Soc. **413**, 262 (2011). https://doi.org/10.1111/j.1365-2966.2010.18130.x. arXiv:1010.3748 [astro-ph.CO]

48. W. Yang, L. Xu, Testing coupled dark energy with large scale structure observation. JCAP **08**, 034 (2014). https://doi.org/10.1088/1475-7516/2014/08/034. arXiv:1401.5177 [astro-ph.CO]

49. J.D. Barrow, T. Clifton, Cosmologies with energy exchange. Phys. Rev. D **73**, 103520 (2006). https://doi.org/10.1103/PhysRevD.73.103520. arXiv:gr-qc/0604063

50. S.A. Bonometto, R. Mainini, M. Mezzetti, Strongly coupled dark energy cosmologies yielding large mass primordial black holes. Mon. Not. R. Astron. Soc. **486**(2), 2321 (2019). https://doi.org/10.1093/mnras/stz846. arXiv:1807.11841 [astro-ph.CO]

51. L. Amendola, J. Rubio, C. Wetterich, Primordial black holes from fifth forces. Phys. Rev. D **97**(8), 081302 (2018). https://doi.org/10.1103/PhysRevD.97.081302. arXiv:1711.09915 [astro-ph.CO]

52. M. Baldi, V. Pettorino, G. Robbers, V. Springel, Hydrodynamical N-body simulations of coupled dark energy cosmologies. Mon. Not. R. Astron. Soc. **403**, 1684 (2010). https://doi.org/10.1111/j.1365-2966.2009.15987.x. arXiv:0812.3901 [astro-ph]

53. E. Carlesi, A. Knebe, G.F. Lewis, S. Wales, G. Yepes, Hydrodynamical simulations of coupled and uncoupled quintessence models. I. Halo properties and the cosmic web. Mon. Not. R. Astron. Soc. **439**(3), 2943 (2014). arXiv:1401.5005 [astro-ph.CO]. https://academic.oup.com/mnras/article/439/3/2943/1105663

54. A.W. Jibrail, P.J. Elahi, G.F. Lewis, Cosmological signatures of dark sector physics: the evolution of haloes and spin alignment. Mon. Not. R. Astron. Soc. **492**(2), 2369 (2020). https://doi.org/10.1093/mnras/stz3606. arXiv:1912.10595 [astro-ph.CO]

55. S. Savastano, L. Amendola, J. Rubio, C. Wetterich, Primordial dark matter halos from fifth forces. Phys. Rev. D **100**(8), 083518 (2019). https://doi.org/10.1103/PhysRevD.100.083518. arXiv:1906.05300 [astro-ph.CO]

56. B. L'Huillier, H.A. Winther, D.F. Mota, C. Park, J. Kim, Dark matter haloes in modified gravity and dark energy: interaction rate, small-, and large-scale alignment. Mon. Not. R. Astron. Soc. **468**(3), 3174 (2017). https://doi.org/10.1093/mnras/stx700. arXiv:1703.07357 [astro-ph.CO]

57. A. Mead, C. Heymans, L. Lombriser, J. Peacock, O. Steele, H. Winther, Accurate halo-model matter power spectra with dark energy, massive neutrinos and modified gravitational forces. Mon.

Not. R. Astron. Soc. **459**(2), 1468 (2016). https://doi.org/10.1093/mnras/stw681. arXiv:1602.02154 [astro-ph.CO]

58. M. Baldi, Cold dark matter halos in Multi-coupled Dark Energy cosmologies: structural and statistical properties. Phys. Dark Univ. **3**, 4 (2014). https://doi.org/10.1016/j.dark.2014.03.001. arXiv:1403.2408 [astro-ph.CO]

59. C. Giocoli, F. Marulli, M. Baldi, L. Moscardini, R. Metcalf, Characterizing dark interactions with the halo mass accretion history and structural properties. Mon. Not. R. Astron. Soc. **434**, 2982 (2013). https://doi.org/10.1093/mnras/stt1218. arXiv:1301.3151 [astro-ph.CO]

60. W.A. Hellwing, M. Cautun, A. Knebe, R. Juszkiewicz, S. Knollmann, Dark Matter haloes as probes of modified gravity. JCAP **10**, 012 (2013). https://doi.org/10.1088/1475-7516/2013/10/012. arXiv:1111.7257 [astro-ph.CO]

61. W. Cui, M. Baldi, S. Borgani, The halo mass function in interacting Dark Energy models. Mon. Not. R. Astron. Soc. **424**, 993 (2012). https://doi.org/10.1111/j.1365-2966.2012.21267.x. arXiv:1201.3568 [astro-ph.CO]

62. E.R. Tarrant, C. van de Bruck, E.J. Copeland, A.M. Green, Coupled quintessence and the halo mass function. Phys. Rev. D **85**, 023503 (2012). https://doi.org/10.1103/PhysRevD.85.023503. arXiv:1103.0694 [astro-ph.CO]

63. W. Yang, S. Vagnozzi, E. Di Valentino, R.C. Nunes, S. Pan, D.F. Mota, Listening to the sound of dark sector interactions with gravitational wave standard sirens. JCAP **07**, 037 (2019). https://doi.org/10.1088/1475-7516/2019/07/037. arXiv:1905.08286 [astro-ph.CO]

64. R.R. Bachega, A.A. Costa, E. Abdalla, K. Fornazier, Forecasting the interaction in dark matter–dark energy models with standard sirens from the Einstein telescope. JCAP **05**, 021 (2020)

65. H. Li, D. He, J. Zhang, X. Zhang, Quantifying the impacts of future gravitational-wave data on constraining interacting dark energy. JCAP **06**, 038 (2020)

66. J. Mifsud, C. van de Bruck, An interacting dark sector and the implications of the first gravitational-wave standard siren detection on current constraints. Mon. Not. R. Astron. Soc. **487**(1), 900 (2019). https://doi.org/10.1093/mnras/stz1293

67. R. Fardon, A.E. Nelson, N. Weiner, Dark energy from mass varying neutrinos. JCAP **0410**, 005 (2004). https://doi.org/10.1088/1475-7516/2004/10/005. arXiv:astro-ph.CO/0309800

68. R.D. Peccei, Neutrino models of dark energy. Phys. Rev. D **71**, 023527023527 (2005). https://doi.org/10.1103/PhysRevD.71.023527. arXiv:hep-ph/0411137

69. X.J. Bi, B. Feng, H. Li, X. Zhang, Cosmological evolution of interacting dark energy models with mass varying neutrinos. Phys. Rev. D **72**, 123523 (2005). https://doi.org/10.1103/PhysRevD.72.123523. arXiv:hep-ph/0412002

70. S. Nojiri, S.D. Odintsov, S. Tsujikawa, Properties of singularities in (phantom) dark energy universe. Phys. Rev. D **71**, 063004 (2005). https://doi.org/10.1103/PhysRevD.71.063004. arXiv:hep-th/0501025

71. M. Khurshudyan, R. Myrzakulov, Late time attractors of some varying Chaplygin gas cosmological models. Symmetry **13**(5), 769 (2021). arXiv:1509.07357 [gr-qc]. https://www.mdpi.com/2073-8994/13/5/769

72. H.B. Benaoum, Accelerated universe from modified Chaplygin gas and tachyonic fluid (2002). arXiv:hep-th/0205140

73. K. Bamba, S. Capozziello, S. Nojiri, S.D. Odintsov, Dark energy cosmology: the equivalent description via different theoretical models and cosmography tests. Astrophys. Space Sci. **342**, 155–228 (2012). https://doi.org/10.1007/s10509-012-1181-8. arXiv:1205.3421 [gr-qc]

74. R.C. Nunes, E.M. Barboza, Dark matter–dark energy interaction for a time-dependent EoS parameter. Gen. Relativ. Gravit. **46**, 1820 (2014). arXiv:1404.1620

75. K. Bamba, S. Capozziello, S. Nojiri, S.D. Odintsov, Dark energy cosmology: the equivalent description via different theoretical models and cosmography tests. Astrophys. Space Sci. **342**, 155 (2012). https://doi.org/10.1007/s10509-012-1181-8. arXiv:1205.3421 [gr-qc]

76. J. Khoury, A. Weltman, Chameleon fields: awaiting surprises for tests of gravity in space. Phys. Rev. Lett. **93**, 171104 (2004). https://doi.org/10.1103/PhysRevLett.93.171104. arXiv:astro-ph/0309300

77. J. Khoury, A. Weltman, Chameleon cosmology. Phys. Rev. D **69**, 044026 (2004). https://doi.org/10.1103/PhysRevD.69.044026. arXiv:astro-ph/0309411

78. D.J. Gross, F. Wilczek, Ultraviolet behavior of nonabelian gauge theories. Phys. Rev. Lett. **30**, 1343 (1973). https://doi.org/10.1103/PhysRevLett.30.1343

79. H.D. Politzer, Reliable perturbative results for strong interactions? Phys. Rev. Lett. **30**, 1346 (1973). https://doi.org/10.1103/PhysRevLett.30.1346

80. M.C. Bento, O. Bertolami, A.A. Sen, Generalized Chaplygin gas, accelerated expansion and dark energy matter unification. Phys. Rev. D **66**, 043507 (2002). https://doi.org/10.1103/PhysRevD.66.043507. arXiv:gr-qc/0202064

81. F. Melia, M.K. Yennapureddy, Model selection using cosmic chronometers with Gaussian processes. JCAP **1802**, 034 (2018). https://doi.org/10.1088/1475-7516/2018/02/034. arXiv:1802.02255 [astro-ph.CO]

82. R.C. Nunes, S. Pan, E.N. Saridakis, New constraints on interacting dark energy from cosmic chronometers. Phys. Rev. D **94**(2), 023508 (2016). https://doi.org/10.1103/PhysRevD.94.023508. arXiv:1605.01712 [astro-ph.CO]

83. H. Stephani, D. Kramer, M. MacCallum, C. Hoensealers, E. Herlt, *Exact Solutions of Einstein's Field Equations* (Cambridge University Press, Cambridge, 2002)

84. A.Y. Kamenshchik, U. Moschella, V. Pasquier, An alternative to quintessence. Phys. Lett. B **511**, 265 (2001). https://doi.org/10.1016/S0370-2693(01)00571-8. arXiv:gr-qc/0103004

85. J. Lu, L. Xu, J. Li, B. Chang, Y. Gui, H. Liu, Constraints on modified Chaplygin gas from recent observations and a comparison of its status with other models. Phys. Lett. B **662**, 87–91 (2008). https://doi.org/10.1016/j.physletb.2008.03.005. arXiv:1004.3364 [astro-ph.CO]

86. A.M. Velasquez-Toribio, M.L. Bedran, Fitting cosmological data to the function $q(z)$ from GR theory: modified Chaplygin gas. Braz. J. Phys. **41**, 59 (2011). https://doi.org/10.1007/s13538-011-0012-7. arXiv:1006.4198 [astro-ph.CO]

87. J. Lu, L. Xu, Y. Wu, M. Liu, Combined constraints on modified Chaplygin gas model from cosmological observed data: Markov Chain Monte Carlo approach. Gen. Relativ. Gravit. **43**, 819 (2011). https://doi.org/10.1007/s10714-010-1103-4. arXiv:1105.1870 [astro-ph.CO]

88. L. Xu, Y. Wang, H. Noh, Modified Chaplygin gas as a unified dark matter and dark energy model and cosmic constraints. Eur. Phys. J. C **72**, 1931 (2012). https://doi.org/10.1140/epjc/s10052-012-1931-3. arXiv:1204.5571 [astro-ph.CO]

89. C. Armendariz-Picon, T. Damour, V.F. Mukhanov, k-inflation. Phys. Lett. B **458**, 209 (1999). https://doi.org/10.1016/S0370-2693(99)00603-6. arXiv:hep-th/9904075

90. J. Garriga, V.F. Mukhanov, Perturbations in k-inflation. Phys. Lett. B **458**, 219 (1999). https://doi.org/10.1016/S0370-2693(99)00602-4. arXiv:hep-th/9904176

91. U. Debnath, A. Banerjee, S. Chakraborty, Role of modified Chaplygin gas in accelerated universe. Class. Quantum Gravity **21**, 5609 (2004). https://doi.org/10.1088/0264-9381/21/23/019. arXiv:gr-qc/0411015

92. J.D. Barrow, String-driven inflationary and deflationary cosmological models. Nucl. Phys. B **310**, 743 (1988). https://doi.org/10.1016/0550-3213(88)90101-0

93. B. Wang, E. Abdalla, F. Atrio-Barandela, D. Pavon, Dark matter and dark energy interactions: theoretical challenges, cosmological implications and observational signatures. Rept. Prog. Phys. **79**(9), 096901 (2016). https://doi.org/10.1088/0034-4885/79/9/096901. arXiv:1603.08299 [astro-ph.CO]

94. Y.L. Bolotin, A. Kostenko, O.A. Lemets, D.A. Yerokhin, Cosmological evolution with interaction between dark energy and dark matter. Int. J. Mod. Phys. D **24**(03), 1530007 (2014). https://doi.org/10.1142/S0218271815300074. arXiv:1310.0085 [astro-ph.CO]

95. C. Wetterich, The Cosmon model for an asymptotically vanishing time dependent cosmological constant. Astron. Astrophys. **301**, 321 (1995). arXiv:hep-th/9408025. http://adsabs.harvard.edu/full/1995A%60%6026A...301..321W

96. L. Amendola et al. (Euclid Theory Working Group), Cosmology and fundamental physics with the Euclid satellite. Living Rev. Relativ. **16**, 6 (2013). https://doi.org/10.12942/lrr-2013-6. arXiv:1206.1225 [astro-ph.CO]

97. D. Pavon, B. Wang, Le Châtelier–Braun principle in cosmological physics. Gen. Relativ. Gravit. **41**, 1 (2009). https://doi.org/10.1007/s10714-008-0656-y. arXiv:0712.0565 [gr-qc]

98. V. Salvatelli, N. Said, M. Bruni, A. Melchiorri, D. Wands, Indications of a late-time interaction in the dark sector. Phys. Rev. Lett. **113**, 181301 (2014). https://doi.org/10.1103/PhysRevLett.113.181301. arXiv:1406.7297 [astro-ph.CO]

99. H. Wei, Cosmological evolution of quintessence and phantom with a new type of interaction in dark sector. Nucl. Phys. B **845**, 381 (2011). https://doi.org/10.1016/j.nuclphysb.2010.12.010. arXiv:1008.4968 [gr-qc]

100. E. Abdalla, L.R.W. Abramo, L. Sodre Jr., B. Wang, Signature of the interaction between dark energy and dark matter in galaxy clusters. Phys. Lett. B **673**, 107 (2009). https://doi.org/10.1016/j.physletb.2009.02.008. arXiv:0710.1198 [astro-ph]

101. E. Abdalla, L.R. Abramo, J.C.C. de Souza, Signature of the interaction between dark energy and dark matter in observations. Phys. Rev. D **82**, 023508 (2010). https://doi.org/10.1103/PhysRevD.82.023508. arXiv:0910.5236 [gr-qc]

102. M.B. Hoffman, Cosmological constraints on a dark matter–dark energy interaction (2003). arXiv:astro-ph/0307350

103. C.G. Boehmer, G. Caldera-Cabral, R. Lazkoz, R. Maartens, Dynamics of dark energy with a coupling to dark matter. Phys. Rev. D **78**, 023505 (2008). https://doi.org/10.1103/PhysRevD.78.023505. arXiv:0801.1565 [gr-qc]

104. F. Arevalo, A.P.R. Bacalhau, W. Zimdahl, Cosmological dynamics with non-linear interactions. Class. Quantum Gravity **29**, 235001 (2012). https://doi.org/10.1088/0264-9381/29/23/235001. arXiv:1112.5095 [astro-ph.CO]

105. D. Wands, J. De-Santiago, Y. Wang, Inhomogeneous vacuum energy. Class. Quantum Gravity **29**, 145017 (2012). https://doi.org/10.1088/0264-9381/29/14/145017. arXiv:1203.6776 [astro-ph.CO]

106. T. Holsclaw, U. Alam, B. Sanso, H. Lee, K. Heitmann, S. Habib, D. Higdon, Nonparametric dark energy reconstruction from supernova data. Phys. Rev. Lett. **105**, 241302 (2010). https://doi.org/10.1103/PhysRevLett.105.241302. arXiv:1011.3079 [astro-ph.CO]

107. M.J. Zhang, J.Q. Xia, Test of the cosmic evolution using Gaussian processes. JCAP **1612**, 005 (2016). https://doi.org/10.1088/1475-7516/2016/12/005. arXiv:1606.04398 [astro-ph.CO]

108. M. Seikel, C. Clarkson, M. Smith, Reconstruction of dark energy and expansion dynamics using Gaussian processes. JCAP **06**, 036 (2012). https://doi.org/10.1088/1475-7516/2012/06/036. arXiv:1204.2832 [astro-ph.CO]

109. T. Holsclaw, U. Alam, B. Sanso, H. Lee, K. Heitman, S. Habib, D. Higdon, Nonparametric reconstruction of the dark energy equation of state. Phys. Rev. D **82**, 103502 (2010). https://doi.org/10.1103/PhysRevD.82.103502. arXiv:1009.5443 [astro-ph.CO]

110. S. Yahya, M. Seikel, C. Clarkson, R. Maartens, M. Smith, Null tests of the cosmological constant using supernovae. Phys. Rev. D **89**(2), 023503 (2014). https://doi.org/10.1103/PhysRevD.89.023503. arXiv:1308.4099 [astro-ph.CO]

111. M. Seikel, S. Yahya, R. Maartens, C. Clarkson, Using H(z) data as a probe of the concordance model. Phys. Rev. D **86**, 083001 (2012). https://doi.org/10.1103/PhysRevD.86.083001. arXiv:1205.3431 [astro-ph.CO]

112. R. von Marttens, V. Marra, L. Casarini, J. Gonzalez, J. Alcaniz, Null test for interactions in the dark sector. Phys. Rev. D **99**(4), 043521 (2019). https://doi.org/10.1103/PhysRevD.99.043521. arXiv:1812.02333 [astro-ph.CO]

113. V.C. Busti, C. Clarkson, Dodging the dark matter degeneracy while determining the dynamics of dark energy. JCAP **1605**, 008 (2016). https://doi.org/10.1088/1475-7516/2016/05/008. arXiv:1505.01821 [astro-ph.CO]

114. R.G. Cai, Q. Su, On the dark sector interactions. Phys. Rev. D **81**, 103514 (2010). https://doi.org/10.1103/PhysRevD.81.103514. arXiv:0912.1943 [astro-ph.CO]

115. R. von Marttens, L. Casarini, D. Mota, W. Zimdahl, Cosmological constraints on parametrized interacting dark energy. Phys. Dark Univ. **23**, 100248 (2019). https://doi.org/10.1016/j.dark.2018.10.007. arXiv:1807.11380 [astro-ph.CO]

116. W.H. Press, B.P. Flannery, S.A. Teukolsky, W.T. Vetterling, *Numerical Recipes in C: The Art of Scientific Computing*, 2nd edn. (Cambridge University Press, Cambridge, 1992)

117. M.K. Yennapureddy, F. Melia, Cosmological tests with strong gravitational lenses using Gaussian processes. Eur. Phys. J. C **78**, 258 (2018). https://doi.org/10.1140/epjc/s10052-018-5746-8. arXiv:1803.06851 [astro-ph.CO]

118. D.W. Hogg, J. Bovy, D. Lang, Data analysis recipes: fitting a model to data. arXiv:1008.4686 [astro-ph.IM]

119. M. Moresco, R. Jimenez, L. Verde, A. Cimatti, L. Pozzetti, C. Maraston, D. Thomas, Constraining the time evolution of dark energy, curvature and neutrino properties with cosmic chronometers. JCAP **12**, 039 (2016). https://doi.org/10.1088/1475-7516/2016/12/039. arXiv:1604.00183 [astro-ph.CO]

120. H. Li, W. Yang, L. Gai, Astronomical bounds on the modified Chaplygin gas as a unified dark fluid model. A&A **623**, A28 (2019). https://www.aanda.org/articles/aa/abs/2019/03/aa33836-18/aa33836-18.html

121. J.-B. Chen, Z.-Q. Liu, L. Xing, Cosmological constraints on the variable modified Chaplygin gas model by using MCMC approach. IJMPD **24**, 1550059 (2015). https://doi.org/10.1142/S0218271815500595

122. R.M. Wald, *General Relativity* (The University of Chicago Press, Chicago, 1984)

123. R.R. Caldwell, A phantom menace? Phys. Lett. B **545**, 23 (2002). https://doi.org/10.1016/S0370-2693(02)02589-3. arXiv:astro-ph/9908168

124. D. Tretyakova, B. Latosh, S. Alexeyev, Wormholes and naked singularities in Brans–Dicke cosmology. Class. Quantum Gravity **32**(18), 185002 (2015). https://doi.org/10.1088/0264-9381/32/18/185002. arXiv:1504.06723 [gr-qc]

125. S. Capozziello, S. Nojiri, S. Odintsov, Unified phantom cosmology: inflation, dark energy and dark matter under the same standard. Phys. Lett. B **632**, 597–604 (2006). https://doi.org/10.1016/j.physletb.2005.11.012. arXiv:hep-th/0507182

126. S. Nojiri, S.D. Odintsov, Unifying phantom inflation with late-time acceleration: scalar phantom-non-phantom transition model and generalized holographic dark energy. Gen. Relativ. Gravit. **38**, 1285 (2006). https://doi.org/10.1007/s10714-006-0301-6. arXiv:hep-th/0506212

127. S. Nojiri, S.D. Odintsov, H. Stefancic, On the way from matter-dominated era to dark energy universe. Phys. Rev. D **74**, 086009 (2006). https://doi.org/10.1103/PhysRevD.74.086009. arXiv:hep-th/0608168

128. M. Setare, J. Sadeghi, A. Amani, From inflation to acceleration, with phantom and canonical scalar fields in non-flat universe. Phys. Lett. B **666**, 288 (2008). https://doi.org/10.1016/j.physletb.2008.07.087

129. C. Wetterich, Cosmology and the fate of dilatation symmetry. Nucl. Phys. B **302**, 668 (1988). https://doi.org/10.1016/0550-3213(88)90193-9. arXiv:1711.03844 [hep-th]

130. B. Ratra, P.J.E. Peebles, Cosmological consequences of a rolling homogeneous scalar field. Phys. Rev. D **37**, 3406 (1988). https://doi.org/10.1103/PhysRevD.37.3406

131. T. Chiba, T. Okabe, M. Yamaguchi, Kinetically driven quintessence. Phys. Rev. D **62**, 023511 (2000). https://doi.org/10.1103/PhysRevD.62.023511. arXiv:astro-ph/9912463

132. D.M. Xia, S. Wang, Constraining interacting dark energy models with latest cosmological observations. Mon. Not. R. Astron. Soc. **463**(1), 952–956 (2016). https://doi.org/10.1093/mnras/stw2073. arXiv:1608.04545 [astro-ph.CO]

133. C. Armendariz-Picon, V.F. Mukhanov, P.G. Steinhardt, Essentials of *k*-essence. Phys. Rev. D **63**, 103510 (2001). https://doi.org/10.1103/PhysRevD.63.103510. arXiv:astro-ph/0006373

134. V.F. Mukhanov, H.A. Feldmann, R.H. Brandenberger, Theory of cosmological perturbations. Phys. Rep. **215**, 203 (1992). https://www.sciencedirect.com/science/article/abs/pii/037015739290044Z?via%3Dihub

135. D. Bini, A. Geralico, D. Gregoris, S. Succi, Scalar field inflation and Shan-Chen fluid models. Phys. Rev. D **90**, 044021 (2014). https://doi.org/10.1103/PhysRevD.90.044021. arXiv:1401.4846 [gr-qc]

136. M. Kopp, C. Skordis, D.B. Thomas, S. Ilić, The Dark Matter equation of state through cosmic history. Phys. Rev. Lett. **120**, 221102 (2018). https://doi.org/10.1103/PhysRevLett.120.221102. arXiv:1802.09541 [astro-ph.CO]

137. W. Hu, Structure formation with generalized dark matter. Astrophys. J. **506**, 485 (1998). https://doi.org/10.1086/306274. arXiv:astro-ph/9801234